KSCE Journal of Civil Engineering (2013) 17(7):1672-1681

DOI 10.1007/s12205-013-1007-4

Structural Engineering

pISSN 1226-7988, eISSN 1976-3808
www.springer.com/12205

Effect of Shrinkage Restraint on Deflections of Reinforced Self-compacting Concrete Beams

Ilker Kalkan* and Jong-Han Lee**

Received January 4, 2012/Revised 1st: June 23, 2012, 2nd: December 9, 2012/Accepted January 12, 2013

Abstract

This paper presents the results of a study aimed at investigating the effects of restrained shrinkage on the in-plane deflection behavior of reinforced beams cast with self-compacting concrete. The load-deflection data from the tests on two sets of heavily-reinforced concrete beams were analyzed. The first set of beams was made with self-compacting concrete while conventionally vibrated concrete with shrinkage reducing admixture was used in the second set. It was found out that the first set underwent shrinkage cracking at early ages and this cracking caused the member responses of the beams to be closer to the fully-cracked response at the initial stages of loading. The second set of beams was found to have initial responses approximate to the uncracked response and the maximum shrinkage restraint stresses were calculated to be in the order of 20-40% of the modulus of rupture of concrete. The maximum shrinkage-induced restraint stress expressions of the AS 3600-2001, AS 3600-2009, EC2, and CSA A23.3-04 codes were found to underestimate the restraint stresses developed in the first set, yet the estimates from code solutions were in closer agreement with the experimental values in the second set.

Keywords: *shrinkage, self compacting concrete, reinforced concrete beams, deflection, effective moment of inertia, shrinkage reducing admixture*

1. Introduction

Restrained shrinkage cracking is a common problem in concrete structures. The National Cooperative Highway Research Program (NCHRP) study carried out by Krauss and Rogalla (1996) reported that more than 100,000 bridges in US faced early-age cracking. Consequently, research programs (Brown *et al*., 2001; Qiao *et al*., 2010; Wan *et al*., 2010, etc.) were conducted by the Departments of Transportation (DOT) of various states in US to understand the reasons for this cracking and to investigate the mitigation strategies to minimize the restrained shrinkage cracking and its effects on the structure.

Shrinkage cracks form in a concrete member when a source of restraint restrains its free volumetric changes associated with shrinkage. The source of restraint can be internal such as reinforcement and aggregate or external such as formwork and adjoining members. Since reinforcement constitutes an important source of restraint, heavily-reinforced concrete beams are more liable to restrained shrinkage cracking compared to lightly-reinforced concrete beams (usually with a reinforcement ratio of 1%).

Restrained shrinkage plays an essential role not only in the durability but also in the service-load behavior of concrete structures. Restraint to the free shrinkage strains induces additional stresses to a member, which result in the reduction of the cracking moment and flexural rigidity. The reduction in the flexural rigidity increases the deflections of the member, which may cause the deflections at service loads to be critical. The shrinkage-induced restraint stresses are a greater cause of concern in concrete members cast with Self-Compacting Concrete (SCC). Many studies in the literature (Leemann and Hoffmann, 2005; Turcry *et al*., 2006; Turcry and Loukili, 2006; etc.) have shown that SCC has a higher rate and amount of shrinkage and is more vulnerable to early-age shrinkage cracking compared to Conventionally Vibrated Concrete (CVC) due to its higher paste volume, lower aggregate content, and lower bleeding capacity. Consequently, SCC flexural members might be subjected to higher restraint stresses, resulting in more pronounced increases in the service-load deflections. The effect of shrinkage restraint stresses on the in-plane deflection response and service-load behavior of reinforced concrete beams cast with SCC has not been studied extensively in the literature. The only study known to the authors that analyzes the in-plane deflection behavior of reinforced beams cast with SCC was carried out by Sonebi *et al*., (2003), who tested SCC and CVC beams of the same concrete grade. The SCC and CVC beams of the same concrete grade had the same dimensions, longitudinal and transverse reinforcement. The beams had a tensile reinforcement

*Assistant Professor, Dept. of Civil Engineering, Kirikkale University, Kirikkale, Turkey (E-mail: ilkerkalkan@kku.edu.tr)
**Member, Assistant Professor, Dept. of Civil Engineering, Daegu University, Gyeongsan 712-714, Korea (Corresponding Author, E-mail: jonghan@daegu.ac.kr)

ratio of 2%. Sonebi *et al*. (2003) found out that at the same load levels SCC beam had narrower and more closely spaced cracks and slightly higher deflections compared to the CVC beam. The deflection predictions from the ACI 318M-05 (ACI Commttee 318, 2005) solution, which is based on Branson (1965) effective moment of inertia formula, were found to be in close agreement with the experimental deflections of both SCC and CVC beams.

The present study primarily aimed at investigating the effect of shrinkage restraint stresses on the cracking moments and in-plane deflection responses of reinforced concrete beams cast with SCC. For this purpose, the experimental load-deflection curves of two sets of heavily-reinforced concrete beams tested by Kalkan (2009) were examined. In the first set of beams, SCC was used, while the second set of beams was cast with CVC and Shrinkage Reducing Admixture (SRA) was added to concrete. Significant differences between the in-plane load-deflection responses of the two sets were found. The restraint stress expressions of the AS 3600-2001 (SA, 2001), AS 3600-2009 (SA, 2009), EC2 (CEN, 2002), and CSA A23.3-04 (CSA, 2004) concrete codes were found to underestimate the maximum shrinkage-induced restraint stresses in the first set of beams, while more accurately estimating the restraint stresses in the second set of beams.

2. Specimen and Material Details

In the present study, the load-deflection data of two sets of rectangular reinforced concrete beams tested by Kalkan (2009) were analyzed. The test beams were heavily-reinforced so that their flexural capacities significantly exceeded their buckling moments. Beams in the first group had slightly higher reinforcement ratios compared to the ones in the second group. Furthermore, SCC was used in the first group. The first group of beams was observed to undergo significant shrinkage cracking before the tests. In order to minimize, if not eliminate, shrinkage cracking of the beams, CVC was used and Eclipse SRA, produced by Grace Construction Products, was added to the concrete mixes in the second group of beams. The differences between the concrete mixes of the two groups of beams provided the two groups with different in-plane (vertical) load-deflection behaviors, which is the focus of the present study. The beams were simply supported at the ends and subjected to a concentrated load at midspan.

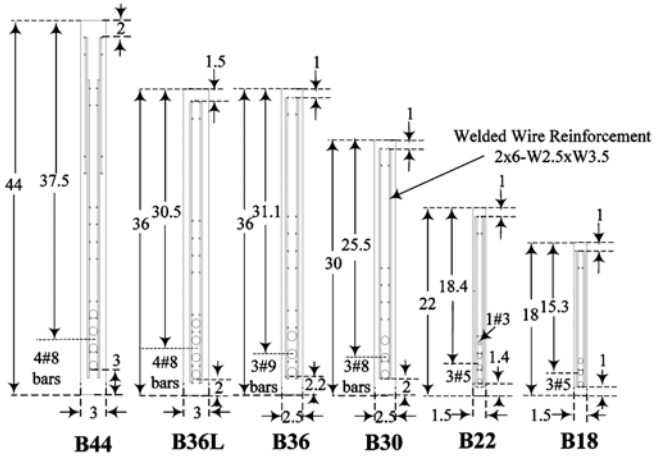

Fig. 1. Reinforcement Details of the Specimens (All Dimensions in Inches, 1 inch = 25.4 mm)

The measured dimensions, reinforcement details and grades, and material properties of the beams are given in Table 1 and Fig. 1. The compressive strength and elastic modulus values tabulated in Table 1 were obtained from cylinder tests carried out according to ASTM C39 and ASTM C469, respectively. Two

Table 1. Details of the Specimens

Group	Beam	$b \times h \times L$ mm (in)	d mm (in)	Longitudinal Rebars	Concrete Mix	ρ%	f'_c MPa (ksi)	E_c MPa (ksi)
I	B18	38 × 457 × 3658 (1.5 × 18 × 144)	362 (14.25)	3#5 Grade 40 [280]	SCC without SRA	3.4	78.1 (11.32)	34450 (5000)
	B22-1	38 × 556 × 3658 (1.5 × 22 × 144)	470 (18.5)	3#5&1#3 Grade 60 [420]	SCC without SRA	3.2	80.9 (11.73)	35800 (5200)
	B22-2	38 × 556 × 3658 (1.5 × 22 × 144)	470 (18.5)	3#5&1#3 Grade 40 [280]	SCC without SRA	3.2	75.8 (11.00)	33400 (4850)
	B30	64 × 762 × 6096 (2.5 × 30 × 240)	648 (25.5)	3#8 Grade 60 [420]	SCC without SRA	3.2	84.3 (12.22)	41000 (5950)
	B36	64 × 914 × 6096 (2.5 × 36 × 240)	787 (31.0)	3#9 Grade 60 [420]	SCC without SRA	3.3	88.1 (12.78)	40350 (5850)
II	B44-1	76 × 1118 × 11887 (3.0 × 44 × 468)	952 (37.5)	4#8 Grade 60 [420]	CVC with SRA	2.4	58.4 (8.47)	30700 (4450)
	B44-2	76 × 1118 × 11887 (3.0 × 44 × 468)	952 (37.5)	4#8 Grade 60 [420]	CVC with SRA	2.4	58.9 (8.54)	30700 (4450)
	B44-3	76 × 1118 × 11887 (3.0 × 44 × 468)	952 (37.5)	4#8 Grade 60 [420]	CVC with SRA	2.4	59.0 (8.56)	31400 (4550)
	B36L-1	76 × 914 × 11887 (3.0 × 36 × 468)	775 (30.5)	4#8 Grade 60 [420]	CVC with SRA	2.9	54.5 (7.90)	29650 (4300)
	B36L-2	76 × 914 × 11887 (3.0 × 36 × 468)	775 (30.5)	4#8 Grade 60 [420]	CVC with SRA	2.9	54.7 (7.94)	31000 (4500)

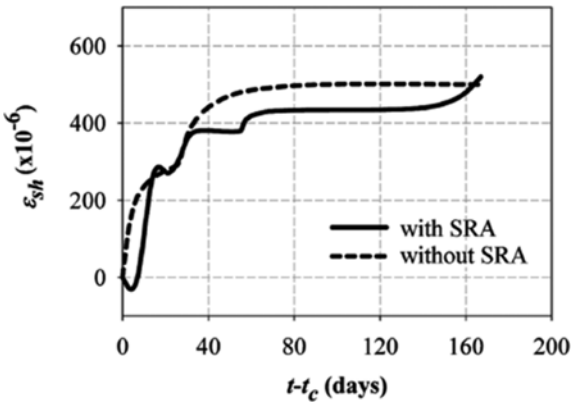

Fig. 2. Free Shrinkage Strains of the Samples from the Concrete of B44

2 × 6-W2.5 × W3.5 sheets, one on each side of the flexural reinforcement, were used in each beam as shear reinforcement shown in Fig. 1. The first set of beams was cured under wet burlaps for a week, while the second set of beams was cured for approximately ten days under synthetic burlene blankets, which are a special type of burlap, whose top surface is covered with polyethylene against rapid drying of the burlap. The concrete mixes of both groups contained Class F fly ash, and low- and high-range water reducing admixtures (LRWR and HRWR) and had a water-cement ratio (w/c) of 0.40. The concrete mixes in the specimens was made using Type I/II Low Alkali cement, a 0.875-in (22-mm) maximum nominal size crushed limestone, and a granitic sand. The concrete mixture contained about 37% coarse aggregate, 27% fine aggregate, 12% cement, and 18% water by volume.

3. Shrinkage Stress Calculations

3.1 Free Shrinkage Strain

Calculation of restraint stress requires the knowledge of the free shrinkage strain of concrete. In the present study, 4 × 4 × 11¼ in. (100 × 100 × 285 mm) prismatic specimens were used to determine the free shrinkage strain of concrete experimentally. Samples were taken from the concrete mixes of beams B44 and B36L according to ASTM C192 and the length changes of the samples were determined according to ASTM C157. Prismatic specimens were taken both prior to and after the addition of SRA's to concrete so that the influence of SRA on the rate and amount of free shrinkage strain could be examined. Free shrinkage strains of samples with and without SRA are compared in Fig. 2, which shows that the amount of strain decreases in the presence of SRA, as previously pointed by several researchers, including Shah *et al*. (1992), Nmai *et al*. (1998), and Gettu *et al*. (2002). Furthermore, Fig. 2 indicates that the rate of shrinkage and the shrinkage at early ages also decrease in the presence of SRA as previously found by various researchers, including Tazawa and Miyazawa (1995) and Berke *et al*. (1997). The decrease in the early-age shrinkage is particularly important considering the fact that formwork may induce major restraint stresses to the beam at early ages. Therefore, the possibility of restrained shrinkage cracking decreases in the presence of SRA in concrete.

For the restraint stress calculations, it was favorable to express the unrestrained shrinkage strain as a function of time via a mathematical expression. For this purpose, the experimental shrinkage strain data obtained from the 4 × 4 × 11¼ in. (100 × 100 × 285 mm) prismatic specimens were compared to four different shrinkage strain models. One of the models is presented in EC2 (CEN, 2002), while the remaining three models are summarized in ACI 209R-08 (ACI Commttee 209, 2008) in detail. The model denoted as ACI 209 is a model introduced in ACI 209R-92 (ACI Commttee 209, 1992) in its final form. The model denoted as GL2000 was originally developed by Gardner and Lockman (2001) and later modified by Gardner (2004). Finally, the model denoted as B3 was developed by Bazant and Baweja (1995). The EC2, B3, and GL2000 models require the knowledge of the 28th-day strength of concrete to estimate the free shrinkage strain. In the present study, the 28th-day strength values of the beams were estimated from the test-day strength values using a strength development model developed by Hwang *et al*. (2004). This model was preferred, since it accounts for the effect of fly ash on the compressive strength development of concrete with time. Concrete with Class F fly ash is known to develop significant strengths at later ages (Gebler and Klieger, 1986).

The main difference between the four models is the time function expressing the change in the free shrinkage strain in time. The free shrinkage strain at a time t $\varepsilon_{sh}(t, t_c)$ is given as:

$$\varepsilon_{sh}(t, t_c) = \varepsilon_{shf} \cdot S(t-t_c) \tag{1}$$

where ε_{shf} is the final (ultimate) free shrinkage strain of concrete; t is the time in days from the cast of concrete; t_c is the duration of curing in days; and $S(t\text{-}t_c)$ is the time function. $t\text{-}t_c$ defines the time from the end of curing, i.e. from the start of drying. In B3 and GL2000 models, ε_{shf} is also multiplied with a correction factor for the effect of ambient relative humidity. In ACI 209 and EC2 models, the time function has the following form:

$$S(t-t_c) = \frac{(t-t_c)}{(t-t_c)+\chi} \tag{2}$$

where χ is a parameter accounting for the shape and size of the member. In both codes, this parameter is a function of the volume-surface ratio of the member, accounting for the surface of the member exposed to drying. Different from Eq. (2), in B3 model the time function is a hyperbolic tangential function:

$$S(t-t_c) = \tanh\sqrt{\frac{t-t_c}{\tau_{sh}}} \tag{3}$$

where τ_{sh} is the shrinkage half-time in days, which is a parameter dependent on the volume-surface ratio and shape of the member. Finally, GL2000 model uses the following form of the time function:

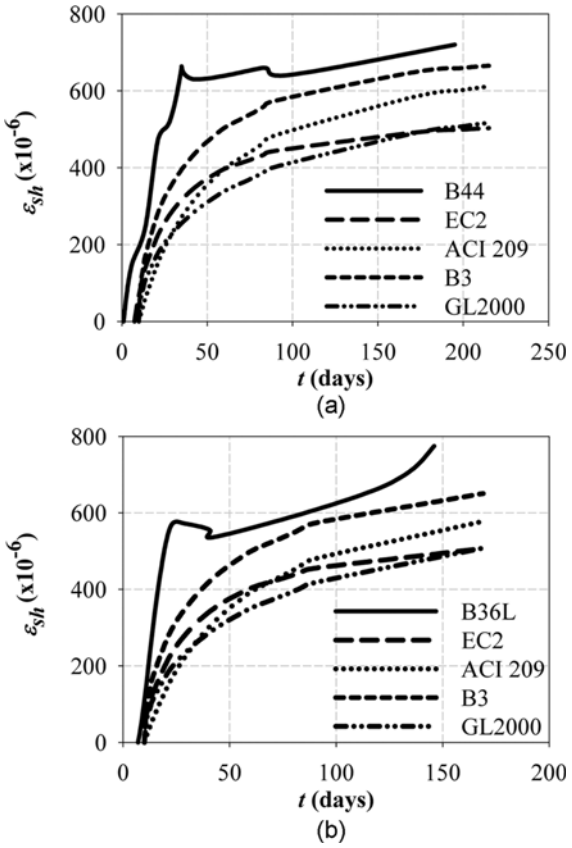

Fig. 3. Comparison of the Analytical Models for Predicting Shrinkage Strains: (a) B44, (b) B36L

$$S(t-t_c) = \left[\frac{(t-t_c)}{(t+t_c)+\chi}\right]^{1/2} \tag{4}$$

where χ depends on the volume-surface ratio of the member.

Different from the data shown in Fig. 2, the experimental data presented in Fig. 3 belong to the shrinkage specimens cured under the same conditions as the beams. Furthermore, these specimens were made from the same concrete mixes (with SRA) as the beams. In this way, the model that best represented the experimental conditions and the beam characteristics could be determined. Fig. 3 shows that B3 model is in closest agreement with the available experimental data. The hyperbolic tangential time function of the B3 model estimated the rapid increase in the shrinkage strain of concrete at early ages, more accurately compared to the remaining three models, which yield to strain estimates significantly lower than the experimental values. Therefore, the B3 model was used for estimating the free shrinkage strain values of the specimens when calculating the restraint stresses.

3.2 Modulus of Rupture of Concrete

Restraint to the shrinkage of concrete induces additional tensile stresses to a beam, denoted as shrinkage restraint stresses. These stresses might cause cracking in the beam if they exceed the tensile strength of concrete. If they remain below the tensile strength of concrete, the beam remains uncracked but its cracking moment decreases due to these stresses. In the context of cracking moment (M_{cr}) and in-plane deflection calculations, the maximum shrinkage-induced restraint stress in a concrete beam (f_{res}) is subtracted from the tensile strength of concrete in flexure (modulus of rupture f_r) to obtain a net (effective) modulus of rupture (f_{re}). This reduction is accounted for in the Australian Concrete Code AS 3600-2009 (SA, 2009) through the following equation:

$$M_{cr} = Z \cdot (f_r - f_{res}) \tag{5}$$

where Z is the section modulus of the uncracked section, referred to the extreme fiber at which cracking occurs; f_r the characteristic flexural tensile strength of concrete; and f_{res} the maximum shrinkage-induced tensile stress on the uncracked section at the extreme fiber at which cracking occurs.

To establish the effect of shrinkage cracking on the cracking moment and in-plane deflections, the modulus of rupture of concrete need to be determined. Two different formulations were used in the present study for this purpose. In several structural concrete codes including ACI 318M-05 (ACI Commttee 318, 2005), CSA A23.3-04 (CSA, 2004), AASHTO-LRFD (AASHTO, 2005), and AS3600-2009 (SA, 2009), the modulus of rupture (f_r) of concrete is calculated from the following equation:

$$f_r = 0.62 \cdot \sqrt{f_c'} \tag{6}$$

where f_c' is the compressive strength of concrete in MPa. The constant 0.62 in the equation slightly changes from code to code. EC2 (CEN, 2002) uses a different formula, given below:

$$f_{ctm,fl} = \max\left[\left(1.6-\frac{h}{1000}\right)\cdot f_{ctm}; f_{ctm}\right] \tag{7}$$

where $f_{ctm,fl}$ is the mean flexural tensile strength in MPa; f_{ctm} the mean axial tensile strength in MPa; h the beam depth in mm. f_{ctm} is obtained from:

$$f_{ctm} = 0.30 \cdot f_{ck}^{2/3} \quad \text{for } f_{ck} \le 50\text{MPa} \tag{8a}$$

$$f_{ctm} = 2.12 \cdot \ln[1+(f_{cm}/10)] \text{ for } f_{ck} > 50\text{MPa} \tag{8b}$$

where f_{ck} and f_{cm} are the characteristic and mean values of the cylinder compressive strength of concrete in MPa, respectively. f_{ck} and f_{cm} are linked according to the following equation:

$$f_{cm} = f_{ck} + 8 \text{ MPa} \tag{9}$$

The strength parameters in the EC2 (CEN, 2002) solution are the 28th-day values. Nevertheless, the tensile strength values at the test day were adopted in the present study instead of the 28th-day values due to the significant differences between the 28th-day and the test-day values. The 28th-day and the test-day values of the mean cylinder compressive strength (f_{cm}) and the mean flexural tensile strength ($f_{ctm,fl}$) are tabulated in Table 2. The f_{cm} values at the test day can be seen to be roughly 20% and 30% greater than the f_{cm} values at the 28th day in the first and second

Table 2. 28th-day and Test-day Strength Values of the Beams

Group	Beam	f_{cm} MPa (ksi)			$f_{ctm,fl}$ MPa (ksi)		
		28th-day	Test day	% Difference	28th-day	Test day	% Difference
I	B18	74.09 (10.74)	91.70 (13.30)	19.2	5.21 (0.75)	5.61 (0.81)	7.4
	B22-1	79.31 (11.50)	94.02 (13.64)	15.6	4.83 (0.70)	5.17 (0.75)	6.6
	B22-2	72.21 (10.47)	87.73 (12.72)	17.7	4.64 (0.67)	5.02 (0.73)	7.6
	B30	77.85 (11.29)	98.24 (14.25)	20.8	4.61 (0.67)	5.05 (0.73)	8.7
	B36	81.73 (11.85)	103.07 (14.95)	20.7	4.70 (0.68)	5.14 (0.74)	8.6
II	B44-1	47.86 (6.94)	65.96 (9.57)	27.4	3.72 (0.54)	4.30 (0.62)	13.5
	B44-2	45.95 (6.66)	66.55 (9.65)	30.9	3.65 (0.53)	4.32 (0.63)	15.5
	B44-3	45.82 (6.65)	66.72 (9.68)	31.3	3.64 (0.53)	4.32 (0.63)	15.9
	B36L-1	44.75 (6.49)	64.04 (9.29)	30.1	3.60 (0.52)	4.24 (0.62)	15.1
	B36L-2	44.71 (6.48)	64.38 (9.34)	30.6	3.60 (0.52)	4.24 (0.62)	15.1

Table 3. Moduli of Rupture of the Beams

Group	Beam	Eq. (6) MPa (ksi)	Eq. (7) MPa (ksi)
I	B18	5.54 (0.80)	5.61 (0.81)
	B22-1	5.60 (0.81)	5.17 (0.75)
	B22-2	5.43 (0.79)	5.02 (0.73)
	B30	5.72 (0.83)	5.05 (0.73)
	B36	5.84 (0.85)	5.14 (0.74)
II	B44-1	4.76 (0.69)	4.30 (0.62)
	B44-2	4.78 (0.69)	4.32 (0.63)
	B44-3	4.78 (0.69)	4.32 (0.63)
	B36L-1	4.60 (0.67)	4.24 (0.62)
	B36L-2	4.60 (0.67)	4.24 (0.62)

set of beams, respectively. These significant differences between the 28th-day and test-day compressive strength values resulted in a roughly 7-8% and 15% difference between the 28th-day and test-day values of $f_{ctm,fl}$ in the first and second set of beams, respectively.

Both formulas, Eqs. (6) and (7), give close values, as tabulated in Table 3. In the following sections, moduli of rupture of the beams are obtained from Eq. (6).

3.3 Restraint Stress

In the present study, the experimental cracking moments of the beams obtained from the load-deflection data were used for obtaining the experimental maximum shrinkage-induced restraint stresses (f_{res}). The load-midspan vertical deflection curves of the first and second groups of beams are illustrated in Figs. 4 and 5, respectively. Fig. 4 indicates that the initial response of each of the first group of beams was closer to the fully-cracked member response rather than the uncracked response. This implies that the maximum shrinkage-induced tensile stress in each of these beams exceeded the tensile strength of concrete, causing the beam to be cracked even before loading. Since the authors deduced that the use of SCC might have caused restrained shrinkage cracking of concrete due to high reinforcement ratios, the shrinkage-induced tensile stresses were reduced in the second group of beams by the use CVC in the beams and by the addition of SRA to concrete. The effect of this change can be observed in Fig. 5, which shows that the initial response of each of the second group of beams was closer to the uncracked response (uncracked transformed or gross section) rather than the fully-cracked response (cracked transformed section). The experimental values of the maximum shrinkage-induced restraint stress of the beams were obtained from the load-deflection data shown in Figs. 4 and 5, using the following formula:

$$f_{res} = f_r - f_{re} \tag{10}$$

where f_r is the modulus of rupture, obtained from Eq. (6), and f_{re} is the effective modulus of rupture, accounting for the shrinkage-induced restraint stresses in the beam. f_{re} is obtained from the following equation:

$$f_{re} = \frac{M_{cr} \cdot \bar{y}}{I_{ucr}} \tag{11}$$

where $\bar{y}$ is the distance from the centroid of the uncracked transformed section to the tension face; and I_{ucr} is the moment of inertia of the uncracked transformed section. Uncracked transformed section properties were used in Eq. (11) instead of gross section properties due to the significant contribution of the reinforcement to the in-plane deflection response of the heavily-reinforced test beams. The uncracked transformed moments of inertia (I_{ucr}) of the beams were calculated to be 15-20% greater than the gross moments of inertia (I_g) of the respective beams. Table 4 tabulates experimental f_{res} values of the test beams together with estimates from different analytical formulations, introduced in the following discussion.

The Australian AS3600 code accounts for the effect of shrinkage-induced restraint from the reinforcement on the cracking moment by the use of Eq. (5). AS3600-2001 (SA, 2001) gives the following relation for f_{res}:

$$f_{res} = \left(\frac{1.5\rho}{1+50\rho}\right) \cdot E_s \cdot \varepsilon_{sh} \tag{12}$$

where ρ is the total longitudinal reinforcement ratio, including both tension and compression reinforcement; E_s is the modulus of elasticity of the longitudinal steel, and ε_{sh} is the free shrinkage

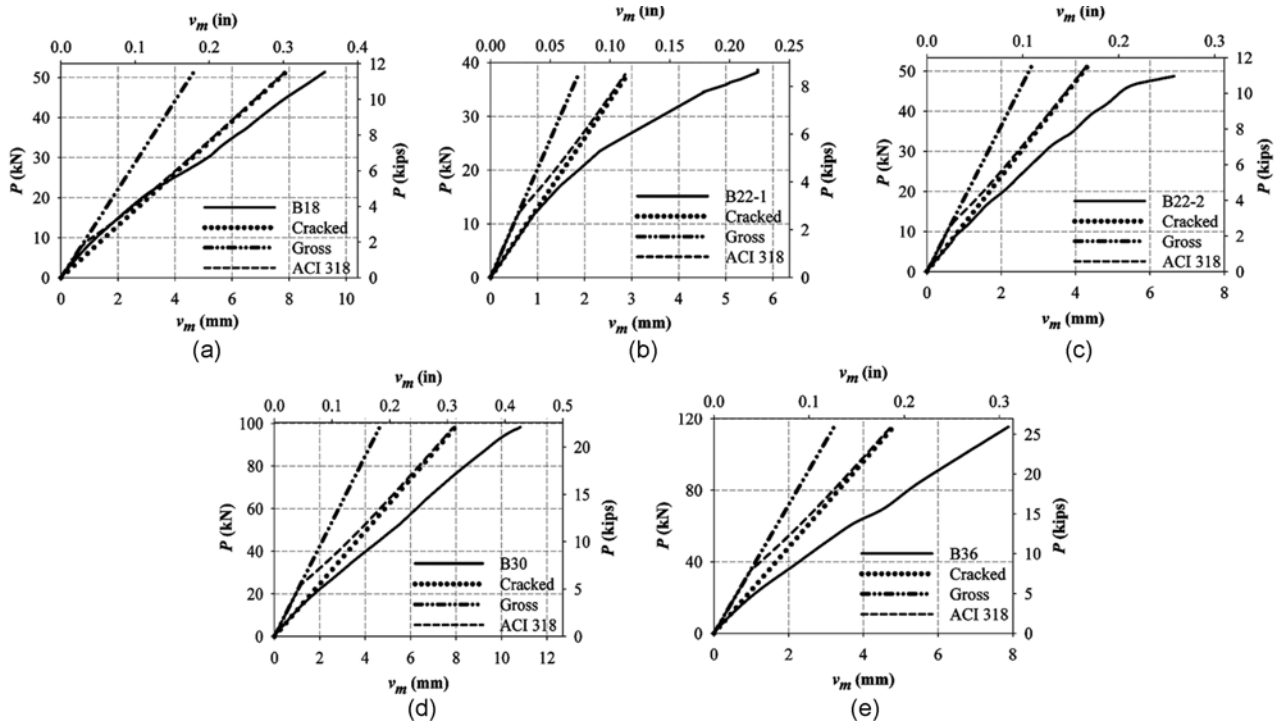

Fig. 4. Load-deflection Curves of the First Group of Beams: (a) B18, (b) B22-1, (c) B22-2, (d) B30, (e) B36

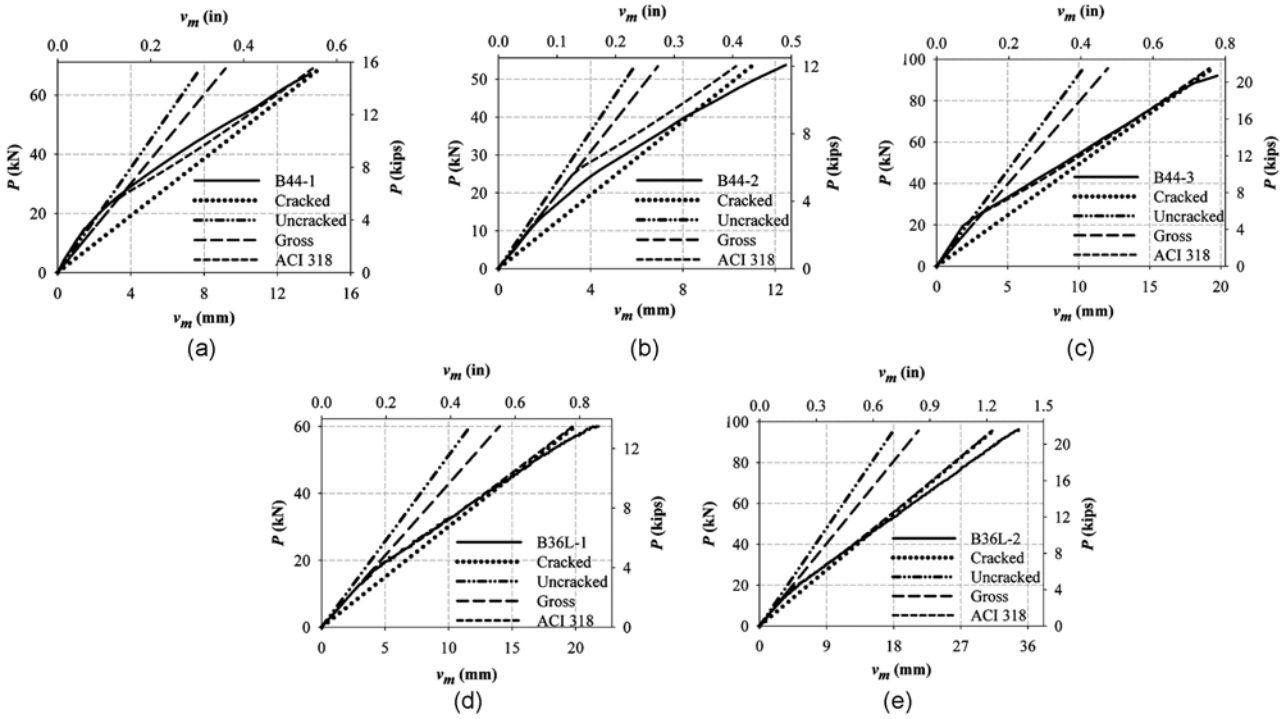

Fig. 5. Load-deflection Curves of the Second Group of Beams: (a) B44-1, (b) B44-2, (c) B44-3, (d) B36L-1, (e) B36L-2

strain of concrete. AS3600-2009 (SA, 2009) gives a different equation for f_{res}, which differentiates between the tension and compression reinforcement:

$$f_{res} = \left(\frac{2.5\rho_w - 0.8\rho_{cw}}{1 + 50\rho_w}\right) \cdot E_s \cdot \varepsilon_{shf} \quad (13)$$

where ρ_w and p_{cw} are the web reinforcement ratios for the tension and compression reinforcement, respectively. The web reinforcement ratios are used in the expression to account for cross-sectional shapes other than rectangular. Eq. (13) also differs from Eq. (12) by the use of the ultimate value of the free shrinkage strain (ε_{shf}), which makes Eq. (13) more conservative. Scanlon

Table 4 . Experimental and Analytical Restraint Stress Values of the Beams

Group	Beam	f_{res}/f_r					
		Experiment	AS3600-2001 (SA, 2001)	AS3600-2009 (SA, 2009)	EC2 (CEN, 2002)	CSA A23.3-04 (CSA, 2004)	Scanlon and Bischoff (2008)
I	B18	1.00	0.42	0.72	0.29	0.47	1.36
	B22-1	1.00	0.38	0.66	0.29	0.47	1.28
	B22-2	1.00	0.38	0.67	0.29	0.47	1.32
	B30	1.00	0.34	0.60	0.29	0.47	1.25
	B36	1.00	0.36	0.63	0.29	0.47	1.33
II	B44-1	0.39	0.49	0.86	0.29	0.46	1.51
	B44-2	0.19	0.49	0.87	0.29	0.46	1.49
	B44-3	0.32	0.49	0.87	0.29	0.46	1.49
	B36L-1	0.21	0.58	1.00	0.28	0.46	1.82
	B36L-2	0.30	0.55	1.00	0.28	0.49	1.78

and Bischoff (2008) proposed the following relation for f_{res}:

$$f_{res} = \left[\frac{\rho \cdot \left(\frac{d}{h}\right) \cdot (1 + 6\xi)}{1 + \overline{n} \cdot \rho \cdot \left(\frac{d}{h}\right) \cdot (1 + 12\xi^2)} \right] \cdot E_s \cdot \varepsilon_{sh} \quad (14)$$

where d is the effective depth; h is the overall beam depth; and $\overline{n}$ is the long-term modular ratio of steel to concrete. In the long-term modular ratio, the decrease in the modulus of elasticity of concrete over time due to creep is taken into account. In the present study, the beams were not loaded until the test day, meaning that creep did not take place in concrete and the shrinkage-induced restraint stresses were not affected from creep. Therefore, the long-term modular ratio in the expression was replaced with the modular ratio n in the calculations. ξ is defined as the eccentricity factor by Scanlon and Bischoff (2008), which the ratio of the eccentricity of reinforcement from the centroid of gross section to the overall depth. By assuming that $d/h = 0.85$ and $\overline{n} = 20$ for a typical reinforced concrete beam, Scanlon and Bischoff (2008) simplified Eq. (14) to the following expression:

$$f_{res} = \frac{2.635\rho \cdot E_s \cdot \varepsilon_{sh}}{1 + 42\rho} \quad (15)$$

Scanlon and Murray (1982) proposed that f_{res} has a value in the order of half of f_r , calculated from Eq. (6). Similarly, the Canadian Concrete Code A23.3-04 (CSA, 2004) assigns a value in the order of half of the rupture modulus calculated from Eq. (6) to the effective modulus of rupture (f_{re}) in the deflection calculations of two-way slabs. Finally, EC2 (CEN, 2002) prescribes a 50% reduction in the tension stiffening when calculating the long-term deflections of concrete beams, accounting for the decrease in the stiffness in time. This reduction corresponds to a reduction of approximately 30% in the modulus of rupture.

Table 4 indicates that there is a clear distinction between the restraint stresses that developed in the first and second groups of beams prior to the tests. The maximum shrinkage-induced restraint stresses (f_{res}) were in the order of 20-40% of the moduli of rupture of concrete (f_r), calculated from Eq. (6), in the second set of beams. On the other hand, f_{res} exceeded f_r in the first set of beams. The analytical estimates from the code solutions (AS, 3600-2001; AS, 3600-2009; EC2 and CSA, A23.3-04) are significantly lower than the experimental values in the first set of beams and the equation proposed by Scanlon and Bischoff (2008) yields to f_{res} estimates in closer agreement with the experimental values. In the second set of beams, on the other hand, the code estimates are in closer agreement with the experimental values with EC2 code solution providing the closest agreement. The equation proposed by Scanlon and Bischoff (2008) significantly overestimates the experimental values. To summarize, the code solutions were found to underestimate the restraint stresses that develop in heavily-reinforced concrete beams made with SCC, while closely estimating the restraint stresses that develop in heavily-reinforced concrete beams made with CVC containing SRA. In the case of heavily-reinforced SCC beams, the solution proposed by Scanlon and Bischoff (2008) more accurately estimates the shrinkage-induced restraint stresses.

The primary reason for the expression of Scanlon and Bischoff (2008) producing estimates much higher than the estimates from the code solutions is the use of the modular ratio (n) in the calculations instead of the long-term modular ratio ($\overline{n}$). As given in Eq. (15), the expression of Scanlon and Bischoff (2008) is originally very similar to the restraint stress expressions of AS3600 codes (Eq. (12) and Eq. (13)) when the effect of creep on the modulus of elasticity of concrete is considered. The equations given in AS3600-2001 and AS3600-2009 are based on the assumption that creep takes place and the shrinkage-induced restraint stresses are affected from creep. This assumption causes the values calculated from the AS3600 code solutions to be significantly smaller than the values calculated from the expression of Scanlon and Bischoff (2008) when creep does not take place. Among the code solutions, the solution of AS3600-2009 (SA, 2009) yields to the highest estimates, while the solution of the EC2 (CEN, 2002) code yields to the lowest estimates.

4. Effective Moment of Inertia and In-plane Deflections

Bending moments exceeding the cracking moment cause discrete flexural cracks to form in the tension zone of a concrete beam. The formation and propagation of these cracks result in the gradual reduction of the overall moment of inertia of a beam from the uncracked moment of inertia (I_{ucr}) to the fully-cracked moment of inertia (I_{cr}). The concrete in the tension zone ceases to contribute to the flexural rigidity at discrete crack locations while the tension-zone concrete between the cracks still contributes to the overall flexural rigidity of the beam. This contribution is known as tension stiffening and it decreases as new cracks form along the span and existing cracks continue to grow and propagate. The tension stiffening results in a gradual transition from the uncracked to the cracked moment of inertia and this gradual transition is accounted for by the use of effective moment of inertia (I_e). Many structural concrete codes including ACI 318M-05 (ACI, 2005), CSA A23.3-04 (CSA, 2004), AASHTO-LRFD (AASHTO, 2005), and AS3600-2009 (SA, 2009) adopt the following effective moment of inertia expression, which was originally developed by Branson (1965):

$$I_e = \left(\frac{M_{cr}}{M_a}\right)^3 \cdot I_g + \left[1 - \left(\frac{M_{cr}}{M_a}\right)^3\right] \cdot I_{cr} \tag{16}$$

where M_a is the maximum moment in the beam. Although being adopted by several codes, recent studies (Bischoff, 2005, 2007; Bischoff and Scanlon, 2007) have shown that Eq. (16) overestimates the stiffness of lightly-reinforced ($\rho < 1\%$) concrete beams and slabs, while providing closer estimates in the case of medium- to heavily-reinforced concrete beams ($\rho > 1\%$). Al-Shaikh and Al-Zaid (1993) found out that the power of the tension-stiffening term $(M_{cr}/M_a)^3$ depends on the reinforcement ratio and proposed that the power 3 should be replaced with $m = 3 - 0.8\rho$.

Equation (16) averages the rigidities of the uncracked and fully-cracked portions of a concrete beam. EC2 (CEN, 2002) and BS 8110-2 (BSI, 1985) adopt a different concept in the deflection calculations, which is based on averaging the flexibilities rather than the rigidities of the uncracked and cracked portions. Following the same concept, Bischoff (2005) proposed the following effective moment of inertia expression:

$$\frac{1}{I_e} = \left(\frac{M_{cr}}{M_a}\right)^2 \cdot \frac{1}{I_g} + \left[1 - \left(\frac{M_{cr}}{M_a}\right)^2\right] \cdot \frac{1}{I_{cr}} \tag{17}$$

Subsequent studies (Gilbert, 2006; Bischoff, 2007; Bischoff and Scanlon, 2007) have indicated that Eq. (17) provides closer estimates to the experimental values in lightly-reinforced concrete beams and slabs and FRP-reinforced concrete beams.

In the present study, the moments of inertia (I_{exp}) of the beams obtained from the experimental load deflection data through Eq. (18) were compared to the analytical I_e values calculated from Eq. (16) and Eq. (17).

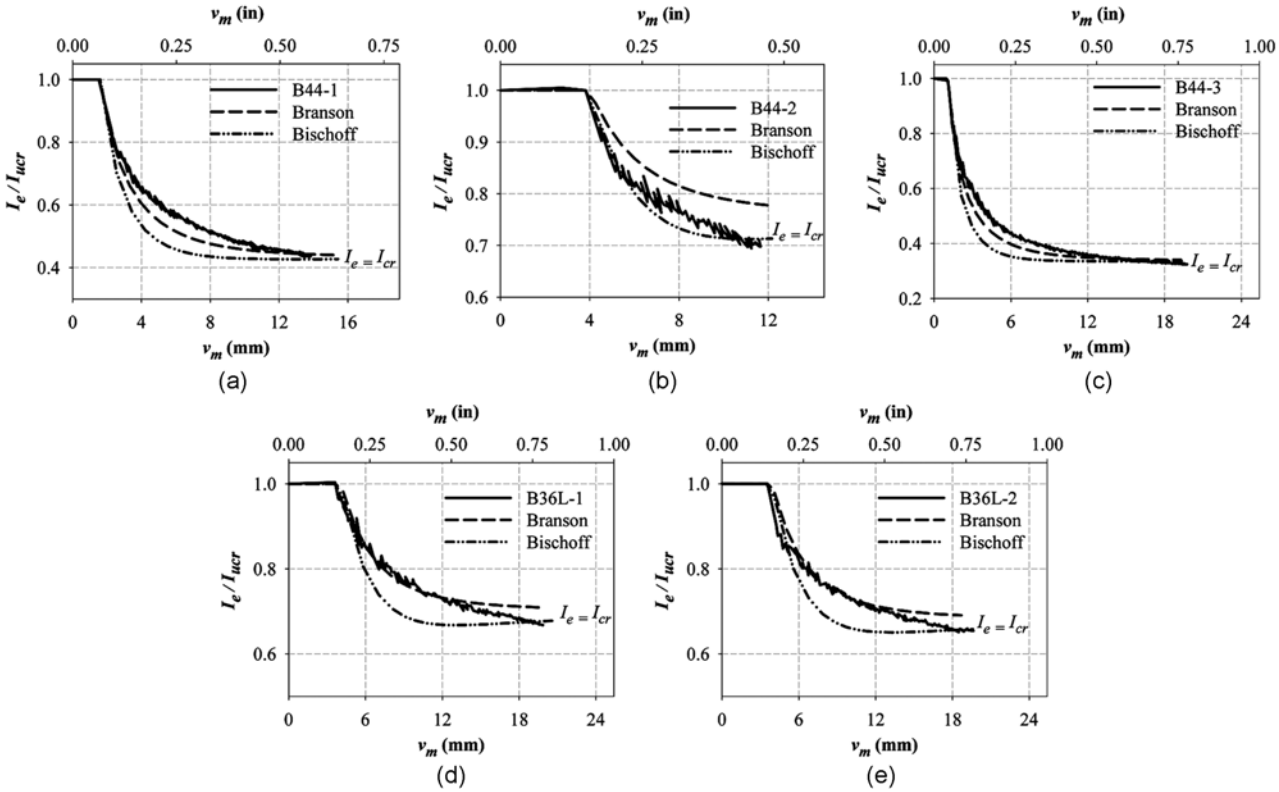

Fig. 6. Effective Moments of Inertia of the Second Group of Beams: (a) B44-1, (b) B44-2, (c) B44-3, (d) B36L-1, (e) B36L-2

$$I_{exp} = \frac{P \cdot L^3}{48 E_c \cdot v_m} \quad (18)$$

where P is the applied load; L is the span length; E_c is the modulus of elasticity of concrete at the test day from the cylinder tests; and v_m is the measured midspan vertical deflection. Since the first group of beams was found to have fully-cracked response at the start of loading due to shrinkage cracking, the comparison was done only for the second group of beams. Fig. 6 shows that Eq. (17) gives smaller I_e estimates compared to Eq. (16). Both I_e expressions (Eqs. (16) and (17)) yielded to estimates in good agreement with I_{exp} values with Branson's expression Eq. (16) being in closer agreement. Bischoff's expression Eq. (17) generally underestimated the I_{exp} values, meaning that the analytical deflection values calculated using Eq. (17) exceeded the measured deflections. In general, both I_e expressions provided satisfactory estimates for the heavily-reinforced test beams, as previously found out by Bischoff (2005, 2007) and Bischoff and Scanlon (2007).

5. Conclusions

The shrinkage-induced restraint stresses and their effect on the in-plane deflection behavior of two sets of heavily-reinforced concrete beams made from two different types of concrete were investigated. The first set of beams was made from Self-Compacting Concrete (SCC). The second set, on the other hand, was made from conventionally vibrated (ordinary) Concrete (CVC), also containing Shrinkage Reducing Admixtures (SRA). The maximum shrinkage-induced restraint stress in each beam was calculated from the experimental load-deflection data and the restraint stress values were compared to the analytical estimates obtained from the restraint stress expressions given in AS 3600-2001 (SA, 2001), AS 3600-2009 (SA, 2009), EC2 (CEN, 2002), and CSA A23.3-04 (CSA, 2004) codes and an expression developed by Scanlon and Bischoff (2008). Furthermore, the moment of inertia of each beam throughout loading was compared to the estimates obtained from two different effective moment of inertia expressions. The following conclusions were drawn:

1. At the initial stages of loading, the experimental load-deflection curves of the beams made with SCC coincided with the lines corresponding to the fully-cracked member response. Accordingly, it was deduced that the maximum shrinkage-induced restraint stresses in the first set of beams exceeded the tensile strength of concrete, causing the beams to be cracked even prior to loading.
2. At the initial stages of loading, the experimental load-deflection curves of the beams made with CVC including SRA coincided with the lines corresponding to the uncracked transformed or gross member response, indicating that the maximum shrinkage-induced restraint stresses in the second set of beams remained below the tensile strength of concrete. The restraint stress values calculated from the experimental cracking moments of the beams indicated that the maximum shrinkage-induced restraint stresses in the second set remained in the order of 20-40 % of the modulus of rupture of concrete before the tests.
3. The restraint stress equations of the AS 3600-2001, AS 3600-2009, EC2, and CSA A23.3-04 codes significantly underestimate the maximum shrinkage-induced restraint stresses that develop in heavily-reinforced concrete beams made with SCC, while providing closer estimates in the case of heavily-reinforced concrete beams made with CVC containing SRA. The estimates from the analytical expression developed by Scanlon and Bischoff (2008) are in closer agreement with the experimental values in heavily-reinforced SCC beams.
4. Both Branson (1965) and Bischoff (2005) effective moment of inertia expressions work well for heavily-reinforced concrete beams. Bischoff effective moment of inertia expression approaches faster to the fully-cracked moment of inertia compared to the Branson expression. Therefore, Bischoff expression produces more conservative estimates.

The use of SCC makes a beam more vulnerable to restrained shrinkage cracking. The problem is emphasized particularly in heavily-reinforced concrete beams, where reinforcement constitutes a significant source of restraint for shrinkage. The possible reductions in the flexural rigidities of heavily-reinforced SCC beams due to restrained shrinkage cracking should be taken into consideration in deflection calculations. The present study indicated that the restrained shrinkage cracking might cause so severe reductions in the flexural rigidities of heavily-reinforced SCC beams that a beam might behave as a fully-cracked member even at the initial stages of loading.

We understand that the findings presented in this paper are dependent on the experimental results of the analyzed beams and that further experimental data may be needed to validate the accuracy of these findings.

References

ACI Committee 209 (1992). *Guide for modeling and calculating shrinkage and creep in hardened concrete*, ACI 209.2R-92, American Concrete Institute, Farmington Hills, Michigan, USA.

ACI Committee 209 (2008). *Guide for modeling and calculating shrinkage and creep in hardened concrete*, ACI 209.2R-08, American Concrete Institute, Farmington Hills, Michigan, USA.

ACI Committee 318 (2005). *Building code requirements for structural concrete and commentary*, ACI 318M-05, American Concrete Institute, Farmington Hills, Michigan, USA.

Al-Shaikh, A. H. and Al-Zaid, R. Z. (1993). "Effect of reinforcement ratio on the effective moment of inertia of reinforced concrete beams." *ACI Structural Journal*, Vol. 90, No. 2, pp. 144-149.

American Association of State Highway and Transportation Officials (AASHTO) (2005). *AASHTO LRFD bridge design specifications (SI Units)*, 3rd Edition, Washington, D.C., USA.

American Society for Testing and Materials (ASTM) (2002). *Standard test method for static modulus of elasticity and poisson's ratio of*

concrete in compression, ASTM C469-02, West Conshohocken, Pennsylvania, USA.

American Society for Testing and Materials (ASTM) (2005). *Standard test method for compressive strength of cylindrical concrete specimens*, ASTM C39/C39M-05, West Conshohocken, Pennsylvania, USA.

American Society for Testing and Materials (ASTM) (2006). *Standard test method for length change of hardened hydraulic-cement mortar and concrete*, ASTM C157/C157M-06, West Conshohocken, Pennsylvania, USA.

American Society for Testing and Materials (ASTM) (2007*). Standard practice for making and curing concrete test specimens in the laboratory*, ASTM C192/C192M-07, West Conshohocken, Pennsylvania, USA.

Bažant, Z. P. and Baweja, S. (1995). "Creep and shrinkage prediction model for analysis and design of concrete structures-Model B3." *Materials and Structures*, Vol. 28, No. 6, pp. 357-365.

Berke, N. S., Dallaire, M. C., Hicks, M. C., and Kerkar, A. (1997). "New developments in shrinkage-reducing admixtures." *Proceedings, 5th International Conference on Superplasticizers and Other Chemical Admixtures in Concrete*, CANMET/ACI, Rome, Italy.

Bischoff, P. H. (2005). "Reevaluation of deflection prediction for concrete beams reinforced with steel and fiber reinforced polymer bars." *ASCE Journal of Structural Engineering*, Vol. 131. No. 5, pp. 752-62.

Bischoff, P. H. (2007). "Rational model for calculating deflection of reinforced concrete beams and slabs." *Canadian Journal of Civil Engineering*, Vol. 34, No. 8, pp. 992-1002.

Bischoff, P. H. and Scanlon, A. (2007). "Effective moment of inertia for calculating deflections of concrete members containing steel reinforcement and fiber-reinforced polymer reinforcement." *ACI Structural Journal*, Vol. 104, No. 1, pp. 68-75.

Branson, D. E. (1965). *Instantaneous and time-dependent deflections of simple and continuous reinforced concrete beams*, HPR Report 7-Part 1, Alabama Highway Department, Bureau of Public Roads, Alabama.

British Standards Institution (BSI) (1985). *Structural use of concrete - Part 2: Code of practice for special circumstances*, BS 8110-2: 1985, London, UK.

Brown, M., Sellers, G., Folliard, K. J., and Fowler, D. W. (2001). *Restrained shrinkage cracking of concrete bridge decks: State-of-the-Art Review*, TxDOT Research Project Report FHWA/TX-0-4098-1, Texas Department of Transportation, Austin, Texas, USA.

Canadian Standards Association (CSA) (2004). *Design of concrete Structures*, A23.3-04, Mississauga, Ontario, Canada.

European Committee for Standardization (CEN) (2002). *Eurocode 2: Design of concrete structures - Part 1: General rules and rules for buildings*, European Standard prEN 1992-1-1, Brussels, Belgium.

Gardner, N. J. (2004). "Comparison of prediction provisions for drying shrinkage and creep of normal strength concretes." *Canadian Journal of Civil Engineering*, Vol. 31, No. 5, pp. 767-775.

Gardner, N. J. and Lockman, M. J. (2001). "Design provisions for drying shrinkage and creep of normal strength concrete." *ACI Materials Journal*, Vol. 98, No. 2, pp. 159-167.

Gebler, S. H. and Klieger, P. (1986). *Effect of fly ash on physical properties of concrete,* ACI SP-91, American Concrete Institute, Farmington Hills, Michigan, USA.

Gettu, R., Roncero, J., and Martin, M. A. (2002). *Study of the behavior of concrete with shrinkage reducing admixtures subjected to long-term drying*, ACI SP-206, American Concrete Institute, Farmington Hills, Michigan, USA.

Gilbert, R. I. (2006). "Discussion of Reevaluation of deflection prediction for concrete beams reinforced with steel and fiber reinforced polymer bars." *ASCE Journal of Structural Engineering*, By Peter H. Bischoff, Vol. 132, No. 8, pp. 1328-1330.

Hwang, K., Noguchi, T., and Tomosawa, F. (2004). "Prediction model of compressive strength development of fly-ash concrete." *Cement and Concrete Research*, Vol. 34, No. 12, pp. 2269-2276.

Kalkan, I. (2009). *Lateral torsional buckling of rectangular reinforced concrete beams*, PhD Thesis, Georgia Institute of Technology, Atlanta, Georgia, USA.

Krauss, P. D. and Rogalla, E. A. (1996). *Transverse cracking in newly constructed bridge decks*, NCHRP Report 380, Transportation Research Board, National Research Council, Washington, D.C., USA.

Leemann, A. and Hoffmann, C. (2005). "Properties of self-compacting and conventional concrete-differences and similarities." *Magazine of Concrete Research*, Vol. 57, No. 6, pp. 315-319.

Nmai, C., Tomita, R., Hondo, F., and Buffenbarger, J. (1998). "Shrinkage reducing admixtures." *Concrete International*, Vol. 20, No. 4, pp. 31-37.

Qiao, P., McLean, D., and Zhuang, J. (2010). *Mitigation strategies for early-age shrinkage cracking in bridge decks*, Washington State Transportation Center Report WA-RD 747.1, Washington State Department of Transportation, Olympia, Washington, D.C., USA.

Scanlon, A. and Bischoff, P. H. (2008). "Shrinkage restraint and loading history effects on deflections of flexural members." *ACI Structural Journal*, Vol. 105, No. 4, pp. 498-506.

Scanlon, A. and Murray, D. W. (1982). "Practical calculation of two-way slab deflections." *Concrete International*, Vol. 4, No. 11, pp. 43-50.

Shah, S. P., Karaguler, M. E., and Sarigaphuti, M. (1992). "Effects of shrinkage-reducing admixtures on restrained shrinkage cracking of concrete." *ACI Materials Journal*, Vol. 89, No. 3, pp. 289-295.

Sonebi, M., Tamimi, A. K., and Bartos, P. J. M. (2003). "Performance and cracking behavior of reinforced beams cast with self-consolidating concrete." *ACI Materials Journal*, Vol. 100, No. 6, pp. 492-500.

Standards Australia (SA) (2001). *Concrete structures*, Australian Standard AS 3600-2001, Standards Australia, Sydney, Australia.

Standards Australia (SA) (2009). *Concrete structures,* Australian Standard AS 3600-2009, Standards Australia, Sydney, Australia.

Tazawa, E. and Miyazawa, S. (1995). "Influence of cement and admixture on autogenous shrinkage of cement paste." *Cement and Concrete Research*, Vol. 25, No. 2, pp. 281-287.

Turcry, P. and Loukili, A. (2006). "Evaluation of plastic shrinkage cracking of self-consolidating concrete." *ACI Materials Journal*, Vol. 103, No. 4, pp. 272-279.

Turcry, P., Loukili, A., Haidar, K., Pijaudier-Cabot, G., and Belarbi, A. (2006). "Cracking tendency of self-compacting concrete subjected to restrained shrinkage: Experimental study and modeling." *ASCE Journal of Materials in Civil Engineering*, Vol. 18, No. 1, pp. 46-54.

Wan, B., Foley, C., and Komp, J. (2010). *Concrete cracking in new bridge decks and overlays*, Wisconsin Highway Research Program Report 10-05, Wisconsin Department of Transportation, Madison, Wisconsin, USA.